

Tuning N,N-Diarylanilinosquaraine Crystal Packing: n-Hexylaryl and Fluoroaryl Substitution

John A. Schlueter,*,† Paul J. Homnick,^{‡,§} Andrea M. Della Pelle,[‡] Paul M. Lahti,*,^{‡,||} and S. Thayumanavan[‡]

[†]Division of Materials Research, National Science Foundation, 2415 Eisenhower Ave, Alexandria, Virginia 22314, United States [‡]Department of Chemistry, University of Massachusetts, Amherst, Massachusetts 01003, United States

Supporting Information

ABSTRACT: X-ray diffraction results for single crystals of N,N-diarylanilinosquaraines (SQ-TAAs) 2,4-bis(4-bis(p-R-phenyl)amino)-2,6-dihydroxyphenyl)cyclobuta-1,3-diene-1,3-bis(olate) for R = F (SQ-TAA-F) and R = n-hexyl (SQ-TAA-C6) are reported. SQ-TAA-F (an ambipolar charge transporter) forms π -stacked dyads intercolated by cross-stacked molecules, a unique motif among the systems studied. Its $[C]-H\cdots F$ contacts induce this intermolecular packing and may account for its ambipolar charge transport behavior. SQ-TAA-C6 (a hole charge transporter) forms strongly slip-stacked 1-D chains aligned along molecular long axes. SQ-TAA-C6 exhibits packing of its conjugated core structure that is similar to those for SQ-TAAs with R = H and R = OH, which also exhibit qualitative

hole transport properties. SQ-TAA-C6 has one *n*-hexyl group that is not fully extended, but all of its alkyl groups pack into alkyl rich planes that alternate with SQ-TAA core rich planes to form the overall lattice.

Squaraine (SQ) dyes are promising building blocks for organic electronic materials, 1 due to their planarized, π -conjugated structures and strong absorption spectra ranging from the lower energy visible into the near-infrared region. N,N-Diarylanilinosquaraines are particularly interesting, with a strong donor—acceptor nature based on a central SQ dye conjugated to peripheral amine units. (For convenience, related structures will be abbreviated as SQ-TAA, squaraine dyes with triarylamines.) Substitution not only influences the molecular electronic properties of such compounds but can affect their crystal packing, which in turn can strongly influence solid state charge carrier mobility. Thompson and co-workers have reported the crystal structure of 2,4-bis(4-(diphenylamino)-2,6-dihydroxyphenyl)cyclobuta-1,3-diene-1,3-bis(olate) (SQ-TAA-H, Chart 1) in organic photovoltaic studies, where

Chart 1. SQ-TAA Compounds

coplanarity of the innermost phenyl rings with the central ring is constrained by intramolecular H-bonding by OH substituents. Thayumanavan and co-workers subsequently reported³ crystallography for 2,4-bis(4-(bis(4-hydroxyphenyl)-amino)-2,6-dihydroxyphenyl)cyclobuta-1,3-diene-1,3-bis-(olate) (SQ-TAA-OH), but otherwise there is a relative dearth of crystallographic information for diarylanilinosquaraines. A search of the Cambridge Structural Database⁴ version 5.39 (November 2017) showed only these two SQ-TAA type structures.

A recent study⁵ described tuning SQ-TAA charge mobility behavior from hole transport through ambipolar to electron transport by substituent variation. But, further crystallographic results were lacking at that time to relate to the observed mobilities. This article now reports single-crystal X-ray diffraction results for two of these SQ-TAA-type compounds with electronically different substitution, electron withdrawing in 2,4-bis(4-(bis(4-fluorophenyl)amino)-2,6-dihydroxyphenyl)cyclobuta-1,3-diene-1,3-bis(olate) (SQ-TAA-F) and mildly electron donating in 2,4-bis(4-(bis(4-hexylphenyl)amino)-2,6-dihydroxyphenyl)cyclobuta-1,3-diene-1,3-bis(olate) (SQ-TAA-C6).

Both SQ-TAA-F and SQ-TAA-C6 were synthesized as described by Della Pelle et al. ⁵ They were allowed to crystallize

Received: October 29, 2018 Revised: May 14, 2019 Published: June 4, 2019

from mixed solvent systems in lightly screw-capped dram vials at ambient temperature, shielded from direct light. SQ-TAA-F yielded small, very dark colored needles. SQ-TAA-C6 produced very thin, green blades (sometimes connected in sheets from which individual blades readily detached): under room lighting, SQ-TAA-C6 often showed highly reflective gold flakes when recrystallized slowly in glass vials (see Supporting Figure S1). For both compounds, single crystals were too thin for diffraction analysis with a typical Mo $K\alpha$ source, so they were analyzed using the Advanced Photon Source at Argonne National Laboratory.

Crystal data and structure refinement information for SQ-TAA-F and SQ-TAA-C6 are given in the endnotes. Supporting Table S1 gives additional data with comparison to previously reported results for SQ-TAA-H and SQ-TAA-OH. All crystallize in monoclinic space groups except for triclinic SQ-TAA-H. SQ-TAA-F has two crystallographically inequivalent molecules per unit cell. The SQ-TAA-OH lattice contains acetone solvate. Figures 1 and 2 show thermal

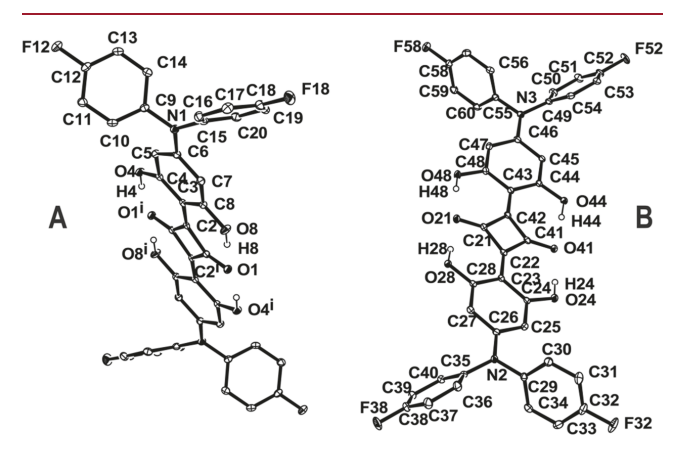


Figure 1. Thermal ellipsoid diagram for SQ-TAA-F at 100 K. Most hydrogen atoms are omitted for ease of viewing. Thermal ellipsoids shown at 30% probability. Form A has inversion center symmetry; form B does not.

Figure 2. Thermal ellipsoid diagram for SQ-TAA-C6 at 100 K. Most hydrogen atoms are omitted for ease of viewing. Thermal ellipsoids shown at 30% probability.

ellipsoid representations for SQ-TAA-F and SQ-TAA-C6, and Supporting Figures S2 and S3 show thermal ellipsoid diagrams

for previously reported SQ-TAA-H² and SQ-TAA-OH³ structures (for comparison).⁷ For discussion purposes, the centrosymmetric molecules in the lattice of SQ-TAA-F are denoted as form A and the others as form B.

All of these compounds are quite similar on the molecular level, as shown by the comparison of select molecular structure parameters in Table 1. All of the central four-atom ring units are held planarized by intramolecular hydrogen bonding with the 2,6-dihydroxyphenyl rings. All of the terminal aryl groups have substantial torsion relative to the diaryl-SQ core—from just over 40° to nearly 80°. In SQ-TAA-C6, three of the hexyl groups are in extended all-anti-staggered conformations, with the fourth having a gauche twist in the middle of the chain (lower left alkyl chain, C61 to C66 in Figure 2), but the molecular structure is otherwise similar to the others. The acetone solvate in the SQ-TAA-OH lattice does not significantly influence the basic molecular conformation.

Given the similar core structures, the substituents (R in Chart 1) terminating the molecular long axes should provide the main influence on intermolecular packing. Figure 3 shows π -stacking for the crystallographic lattices, and Chart 2 schematically shows the major stacking motifs. Figure S4 in the Supporting Information shows analogous down-the-stack pictorial comparisons using structure diagrams. Table 1 lists stack-related packing distances for the SQ-TAA structures; both closest atom-to-atom approaches between four-member rings and plane-to-plane distances between four-member rings are given, since there is substantial slip stacking in some of the structures. The compounds crystallize with essentially parallel molecular long axes, except for SQ-TAA-F in which crystallographic form B forms long-axis-aligned dyads, with form A inserted between dyads but the long-axis rotated roughly 50° to give crossed stacking (see Figure S4b) with a -B-A-B-B-A-B- pattern. For SQ-TAA-F, each B-A-B cross-stacked triad is generated by the inversion center in the A-form molecule. Each B-B dyad is related by an inversion center and has a modest staircase offset with limited slip stacking; the plane-to-plane distance between B-B dyad central four-atom rings is 2.95 Å (distance d in Chart 2). The centroid of the Bform four-member ring is 3.38 Å above/below a plane formed by the four-member ring carbons of the A-form (distance d' in Chart 2).

The notably different packing of SQ-TAA-F forms with an extensive network of [C]-H···F H-bond type interactions. In particular, the cross-stack A-B contact has a [C53]-H53 to F18 donor-acceptor ($[D]H\cdots A$) H-bond of length ~2.6 Å, with a D-H···A angle of 147.40°, plus a [C19]-H19 to F38 ([D]H···A) length of ~ 2.7 Å, with a D-H···A angle of 159.06°. The former contact has the A form as an acceptor; the latter has the B form as an acceptor. Table S2 lists these and other H-bond type contacts in the SQ-TAA-F crystal structure. Figure 4 (and Supporting Figure S5) shows several other H...F contacts. Substituents F12, F18 (A form), and F32 (B form) are each involved in bifurcated H-bonding to aryl C-H bonds of two other molecules (Figure 4), involving both A and B form molecules in each case. Overall, although SQ-TAA-F for geometric reasons would presumably favor stacks with all molecular long axes parallel, the observed cross-stacking gives numerous stabilizing [C]-H···F contacts.

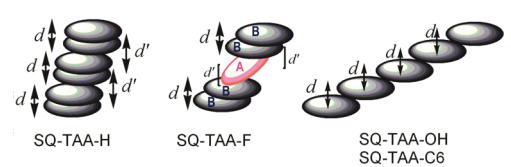
The differences in the other three crystal lattices lie in variable staircase and slip-stack offsets within π -stacks. SQ-TAA-H has alternating intermolecular distances along a stack, ~ 3.3 and ~ 3.6 Å plane-to-plane between the central four-atom

Table 1. Molecular Structure, Intermolecular Packing Parameters, and Charge Mobilities for SQ-TAA Compounds [A and B, Two Crystallographically Inequivalent Molecules in the SQ-TAA-F Structure; Italicized Entries, Values for the Crystallographic B Molecule As Described in the Text]

	SQ-TAA-H	SQ-TAA-OH	SQ-TAA-F	SQ-TAA-C6
Molecular parameters				
rC_{SQ} - N^a (Å)	1.384(7), 1.387(7)	1.370(4)	1.383(3) 1.373, 1.384	1.372(4), 1.370(4)
rC-Ph ^b (Å)	1.410(7), 1.419(7)	1.408(4)	1.405(3) 1.401(3), 1.409(3)	1.400(4), 1.407(4)
r(N-Ph) ^c (Å)	1.437(6), 1.435(6) 1.440(6), 1.426(6)	1.438(4), 1.444(4)	1.433(3), 1.434(3) 1.439(3), 1.441(3) 1.43(3)1, 1.440(3)	1.436(4), 1.446(4) 1.434(4), 1.442(4)
Ph-SQ ^d tors (deg)	1.2-6.9	1.4-3.1	1.8-2.1 0.8-7. <i>I</i>	3.9-7.1
Ph-N-C ^e tors (deg)	50.2, 61.8 49.2, 62.6 R	59.4, 65.0 R	47.3, 58.5° 43.3, 65.8° 47.9, 78.3°	59.6, 59.9 58.1, 60.6
Closest Inter-4-ring contact	OH O	HO R		
SQ···SQ' (Å)	4.14 ^f [3.34 ^g] 4.86 ^{f,h} [3.60 ^{g,h}]	8.13 ^f [3.57 ^g]	$4.19^{\rm f} [2.95^{\rm g}] \\ 3.88^{\rm f,h}$	8.12 ^f [3.66 ^g]
Charge Mobility ⁱ				
Pristine film	$9.6 \times 10^{-4} (h^+)$	$0.19 \times 10^{-4} (h^+)$	$0.022 \times 10^{-4} (h^+)$ $0.011 \times 10^{-4} (e^-)$	$0.042 \times 10^{-4} (h^+)$
Annealed film ^j	5.7×10 ⁻⁴ (h ⁺)	$0.19 \times 10^{-4} (h^+)$	0.052×10 ⁻⁴ (h ⁺) 0.096×10 ⁻⁴ (e ⁻)	25×10 ⁻⁴ (h ⁺)

a^{--e}See diagram to identify bonds and torsions. ^fClosest intermolecular C···C contact between 4-member rings. ^gPlane-to-plane distance between four-member ring cores, using all four carbons of the four-member ring for plane generation. ^hDistance d' in Chart 2: long contact for SQ-TAA-H, A···B contact for SQ-TAA-F. ⁱAll charge mobilities given in units of cm²·V⁻¹·s⁻¹, for hole (h⁺) or electron (e⁻) transport measured using a field effect transistor (FET) method for solution-coated thin film samples on glass, as reported in ref 5. ^jPristine film spin-coated on glass was annealed at 100 °C for 60 min and mobility measurement repeated.

Chart 2. Qualitative Stacking Patterns of SQ-TAA Compounds^a



^a"A" form of SQ-TAA-F is centrosymmetric.

rings (distances *d* and *d'* in Chart 2, respectively). It has only a small staircase offset but is slip-stacked by about 40° to place the center of a four-member ring roughly above a dihydroxyphenyl ring of the molecule below. SQ-TAA-OH molecules have a small staircase offset along a 1-D stack that has a plane-to-plane distance of about 3.57 Å using the central four-member rings. These are much more stack slipped than SQ-TAA-H (Figure 3 and Chart 2), by about 154°, placing each central four-member ring roughly above the terminal 4-hydroxyphenyl rings of the molecule below. SQ-TAA-C6 stacks quite similarly to SQ-TAA-OH, at about 3.66 Å plane-to-plane between central four-member rings, with little

staircase offset but somewhat more slip stacked than SQ-TAA-OH at about 159°, placing each four-member ring roughly above the hexyl groups on the terminal aryl rings of the molecule below it.

The substitution-induced changes in molecular stacking may help explain differences observed in behavior of spin-coated thin film samples of SQ-TAA's, which Della Pelle et al. reported previously. Of course, solution spin-coated films may not have similar intermolecular packing or organization to those of crystals made by slow evaporation. But, comparing the crystal packing results to the thin film behaviors provides permissive evidence and directions for future study. Overall, SQ-TAA-F shows the biggest effect of terminal-aryl substitution on crystallographic packing. Table 1, from results reported previously by Della Pelle et al., shows that SQ-TAA-F also had qualitatively different charge transport behavior, exhibiting (weakly) ambipolar charge transport properties of $\sim 10^{-6}~{\rm cm}^2\cdot{\rm V}^{-1}\cdot{\rm s}^{-1}$. The others exhibited hole carrier transport.

Della Pelle et al. previously noted⁵ that SQ-TAA-F did *not* show a lowest unoccupied molecular orbital (LUMO) level difference relative to the other SQ-TAA's, as would simplistically be expected if *molecular* structure alone causes the difference. But, if the different intermolecular packing in

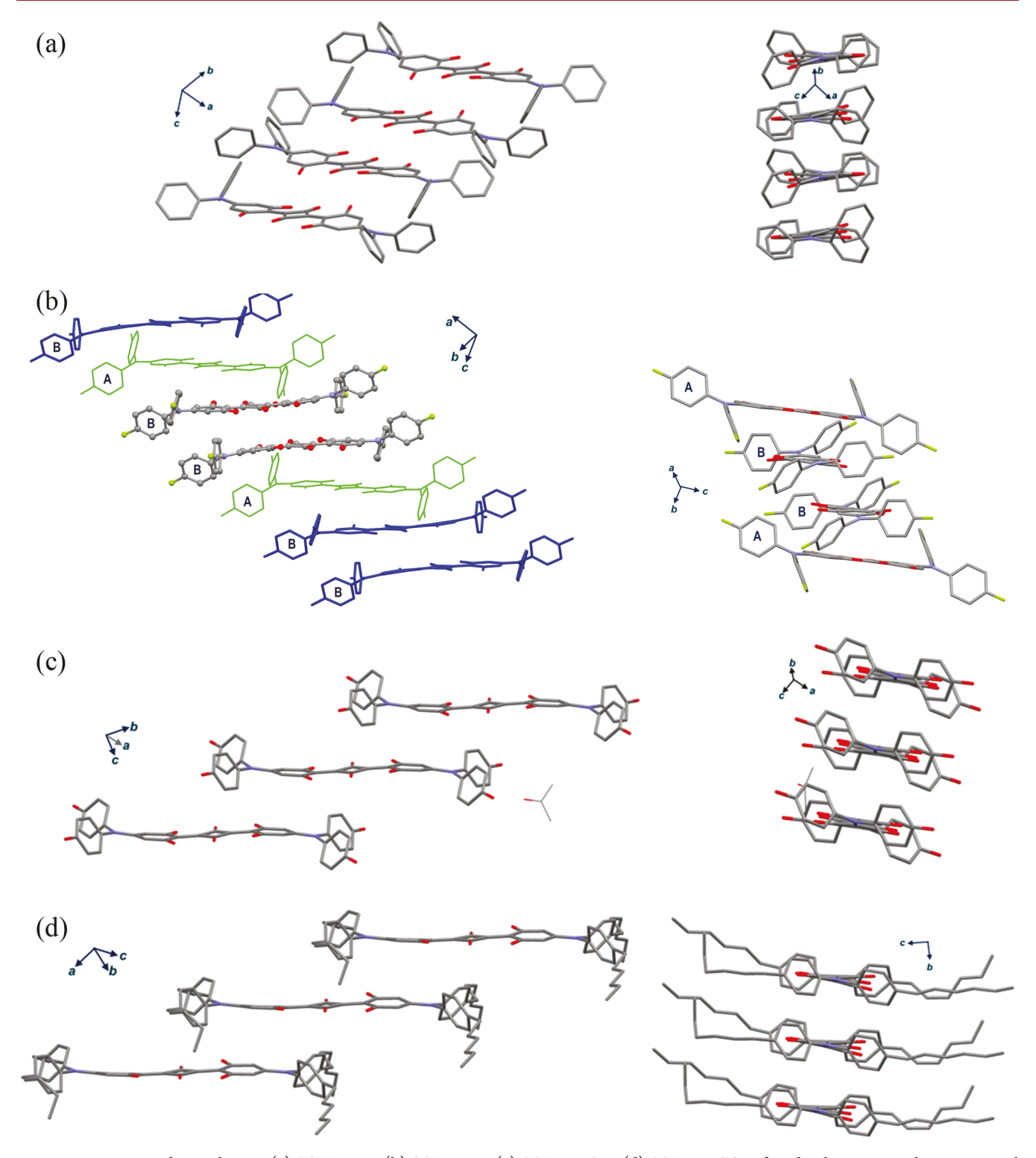


Figure 3. Diagrammed π -stacking in (a) SQ-TAA-H, (b) SQ-TAA-F, (c) SQ-TAA-OH, (d) SQ-TAA-C6. Left and right views are the same crystal structure. Broken arrows in b link the same molecular structures left and right. "A" in diagram b is the centrosymmetric form of SQ-TAA-F. Stick structure in the left-hand part of c is acetone solvate.

SQ-TAA-F reflects similar intermolecular contacts in its spincoated thin films—which we emphasize is just a hypothesis from the available data—such packing differences could help explain why only SQ-TAA-F is ambipolar. As a similar example, a first report of ambipolar charge transport in isoindigo-core conjugated polymers resulted from fluorine substitution: the transport behavior was attributed to fluorine substituent effects on molecular-level electronics *and* intermolecular packing effects (including higher crystalline tendencies).⁸ Although SQ-TAA-F film morphologies are not known here, the single crystal structure shows specific [C]-H··· F interactions that should uniquely influence SQ-TAA-F intermolecular packing compared to the other SQ-TAA, even

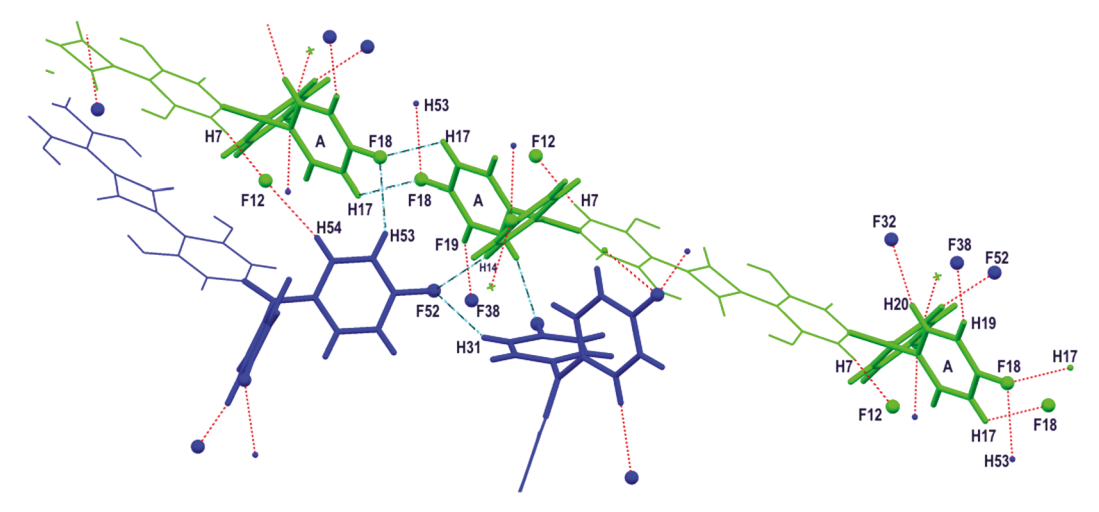


Figure 4. Select H···F contacts in SQ-TAA-F. "A" designates form A (green), centrosymmetric molecules in the lattice. Many atoms are omitted for ease of viewing the contacts. See Supporting Information Table S2 for a listing of H···F contacts and symmetry operations that relate them.

though molecular-level electronic properties are not much changed.

Della Pelle et al. also noted that when the SQ-TAA thin films were annealed at 80 °C for 30 min, SQ-TAA-C6 showed⁵ a 500-fold increase in hole transport, by far the largest annealing-induced change in that study. The annealed SQ-TAA-C6 films also develop a new, sharply distinct, low energy spike in the UV-vis spectrum (Supporting Figure S6), at 12 700 cm⁻¹ (787 nm, 1.58 eV) versus the broad pristine peak maximum at 14 060 cm⁻¹ (711 nm, 1.71 eV). Only SQ-TAA-C6 showed these spectral changes, which suggest the formation of n-extended electronic coupling from intermolecular interaction. The changes resemble low energy spectral bands formed in spin-coating and/or annealing of regionegular poly(3-hexylthiophene-2,5-diyl) (P3HT) films. Such bands are attributable 10 to higher degrees of crystallinity induced by organizing rigid aromatic core structures within a solid and are associated with better electronic performance. 11 The crystal lattice of SQ-TAA-C6 reflects such organization, with alternating zones running parallel to the ab plane that contain the "soft" alkyl side chains and the rigid SQ-TAA cores (see Supporting Figure S7).

But, annealing of single SQ-TAA-C6 crystals under nitrogen at either 79 or 100 °C for 60 min, followed by cooling to ambient temperature, did *not* yield significant changes to the crystallography (see Supporting Information for CCDC Deposition #1916005, Table S1). So, any annealed changes in SQ-TAA-C6 films do not seem to arise from molecular packing changes of putative crystal domains. It seems more likely that—like P3HT and other rigid-core materials with sufficiently long alkyl side chains ^{12,13}—spin-coating SQ-TAA-C6 gives largely amorphous pristine films, which become more organized and crystalline with annealing. Further study would be needed to verify this hypothesis.

In summary, the new crystal structures reported herein for SQ-TAA-F and SQ-TAA-C6 provide intermolecular packing information for members of the electronically promising diarylanilinosquaraines. SQ-TAA-F has quite different crystallography by comparison to the other SQ-TAA compounds discussed herein. SQ-TAA-F alone in this set has ambipolar charge transport behavior, and its different crystal packing is likely to be at least as important for determining charge transport as the isolated-molecule electronic nature might be,

at least for substantially crystalline solid samples. The similarity of SQ-TAA-C6 π -stacking to that of SQ-TAA-H and SQ-TAA-OH indicates that such long-axis-aligned, 1-D stack organization should be strongly favored in similar compounds without fluorine substitution, with modest variation in staircase offsets and slip-stacking being the major substituent-induced crystallographic changes that could influence electronic behavior. The results for SQ-TAA-C6 strongly suggest testing other extended chain substituents on the SQ-TAA core to get high hole transport capability, with different annealing strategies and lattice variation studies as part of the work. Mixed crystal studies involving SQ-TAA-F and similar, partly F-substituted terminal aryl groups in SQ-TAA systems could also be interesting, given the potential influence of differing patterns of H···F interaction in a crystal lattice. Further studies of such molecules are desirable for better correlation and prediction of charge transport properties as a function of their molecular structures.

ASSOCIATED CONTENT

Supporting Information

The Supporting Information is available free of charge on the ACS Publications website at DOI: 10.1021/acs.cgd.8b01621.

Comparison table of crystallographic and structure refinement data for SQ-TAA-H, SQ-TAA-OH, SQ-TAA-F, and SQ-TAA-C6 (including the postannealed data for SQ-TAA-C6); ellipsoid diagrams for SQ-TAA-H and SQ-TAA-OH; selected diagrams of crystal packing; pristine and postannealed thin film UV—vis spectra for SQ-TAA-C6, details of FET charge transport measurement results given in Table 1 (PDF)

Accession Codes

CCDC 1869227–1869228 and 1916005 contain the supplementary crystallographic data for this paper. These data can be obtained free of charge via www.ccdc.cam.ac.uk/data_request/cif, or by emailing data_request@ccdc.cam.ac.uk, or by contacting The Cambridge Crystallographic Data Centre, 12 Union Road, Cambridge CB2 1EZ, UK; fax: +44 1223 336033.

AUTHOR INFORMATION

Corresponding Authors

*E-mail: jschluet@nsf.gov.

*E-mail: lahti@chem.umass.edu.

ORCID ®

Paul M. Lahti: 0000-0003-4255-4733 S. Thayumanavan: 0000-0002-6475-6726

Present Address

§3M Oral Care Solutions Division, 3M Center, St. Paul, MN 55144

Author Contributions

J.A.S. carried out all crystal mounting, annealing, and crystal analysis. P.J.H. crystallized samples of SQ-TAA-F and SQ-TAA-C6. A.M.D.P. synthesized the compounds studied. P.M.L. and S.T. supervised the noncrystallographic work. All authors participated in writing/review of this article.

Notes

The authors declare no competing financial interest. $^{\parallel}$ Emeritus, retired.

ACKNOWLEDGMENTS

The authors (J.A.S.) acknowledge with thanks the use of the Advanced Photon Source at Argonne National Laboratory: NSF's ChemMatCARS Sector 15 is supported by the Divisions of Chemistry (CHE) and Materials Research (DMR), National Science Foundation, under grant number NSF/CHE-1834750. Use of the Advanced Photon Source, an Office of Science User Facility operated for the U.S. Department of Energy (DOE) Office of Science by Argonne National Laboratory, was supported by the U.S. DOE under Contract No. DE-AC02-06CH11357. J.A.S. acknowledges support from the Independent Research/Development (IRD) program while serving at the National Science Foundation. The initial stages of crystallizing samples SQ-TAA-F and SQ-TAA-C6 were carried out at the University of Massachusetts Amherst (P.M.L., P.J.H.), supported by Polymer-Based Materials for Harvesting Solar Energy (PHaSE), an Energy Frontier Research Center, funded by the U.S. Department of Energy (DOE), Office of Science, Office of Basic Energy Sciences (BES), Materials Sciences and Engineering Division under Award # DE-SC0001087. We thank the reviewers for helpful commentary.

REFERENCES

- (1) Chen, G.; Sasabe, H.; Igarashi, T.; Hong, Z.; Kido, J. Squaraine dyes for organic photovoltaic cells. *J. Mater. Chem. A* **2015**, *3*, 14517–14534.
- (2) Wang, S.; Hall, L.; Diev, V. V.; Haiges, R.; Wei, G.; Xiao, X.; Djurovich, P. I.; Forrest, S. R.; Thompson, M. E. N,N-Diarylanilinosquaraines and Their Application to Organic Photovoltaics. *Chem. Mater.* **2011**, 23, 4789–4798.
- (3) Karak, S.; Homnick, P. J.; Della Pelle, A. M.; Bae, Y.; Duzhko, V. V.; Liu, F.; Russell, T. P.; Lahti, P. M.; Thayumanavan, S. Crystallinity and Morphology Effects on a Solvent-Processed Solar Cell Using a Triarylamine-Substituted Squaraine. *ACS Appl. Mater. Interfaces* **2014**, *6*, 11376–11384.
- (4) Groom, C. R.; Bruno, I. J.; Lightfoot, M. P.; Ward, S. C. The Cambridge Structural Database. *Acta Crystallogr., Sect. B: Struct. Sci., Cryst. Eng. Mater.* **2016**, *B72*, 171–179.
- (5) Della Pelle, A. M.; Homnick, P. J.; Bae, Y.; Lahti, P. M.; Thayumanavan, S. Effect of Substituents on Optical Properties and Charge-Carrier Polarity of Squaraine Dyes. *J. Phys. Chem. C* **2014**, *118*, 1793–1799.
- (6) Crystal data for SQ-TAA-F: $C_{40}H_{24}F_4N_2O_6$, FW = 704.61, monoclinic, space group $P2_1/c$, a=15.0986(7) Å, b=16.9594(7) Å, c=18.9745(8) Å, $\beta=101.4777(10)^\circ$, V=4761.5(4) Å³, T=100(2) K, μ (= 0.41328 Å) = 0.045 mm⁻¹, density (calcd) = 1.474 g/cm³, Z=6, F(000)=2172; 97 273 reflections measured, 11 871 independent

- reflections ($R_{\rm int}=0.122$); $R_1=0.0603$, $wR(F^2)=0.1361$ ($I>2\sigma(I)$); $R_1=0.1046$, $wR(F^2)=0.1551$ (all data). The goodness of fit on F^2 was 1.048. Least squares weighting = $1/[/^2(F_o^2)+(0.0464P)^2+5.2555P]$ where $P=(F_o^2+2F_c^2)/3$. CCDC number 1869227. Crystal data for SQ-TAA-C6: $C_{64}H_{72}N_2O_6$, FW = 969.26, monoclinic, space group $P2_1/c$, a=10.0378(7) Å, b=17.2982(14) Å, c=31.145(2) Å, $\beta=97.645(2)^\circ$, V=5359.8(7) ų, T=100(2) K, $\mu(=0.51823$ Å) = 0.019 mm⁻¹, density (calcd) = 1.201 g/cm³, Z=4, F(000)=2088. 10 984 reflections measured, 6194 independent reflections ($R_{\rm int}=0.135$); $R_1=0.0778$, $wR(F^2)=0.1556$ ($I>2\sigma(I)$); $R_1=0.1556$, $wR(F^2)=0.1911$ (all data). The goodness of fit on F^2 was 1.077. Least squares weighting = $1/[/^2(F_o^2)+(0.0565P)^2+7.6952P]$ where $P=(F_o^2+2F_c^2)/3$. CCDC number 1869228.
- (7) Thermal ellipsoid diagrams generated using ORTEP-3 for Windows v. 2013.1; cf. Farrugia, L. J. WinGX and ORTEP for Windows: an update. J. Appl. Crystallogr. 2012, 45, 849–854.
- (8) Lei, T.; Dou, J.-H.; Ma, Z.-J.; Yao, C.-H.; Liu, C.-J.; Wang, J.-Y.; Pei, J. Ambipolar Polymer Field-Effect Transistors Based on Fluorinated Isoindigo: High Performance and Improved Ambient Stability. *J. Am. Chem. Soc.* **2012**, *134*, 20025–20028.
- (9) Cf. an overview and references in: Tremel, K.; Ludwigs, S. Morphology of P3HT in Thin Films in Relation to Optical and Electrical Properties. *Adv. Polym. Sci.* **2014**, 265, 39–82.
- (10) Cf. discussion and references in: Niles, E. T.; Roehling, J. D.; Yamagata, H.; Wise, A. J.; Spano, F. C.; Moulé, A. J.; Grey, J. K. J. Aggregate Behavior in Poly-3-hexylthiophene Nanofibers. *J. Phys. Chem. Lett.* **2012**, *3*, 259–263.
- (11) McDowell, C.; Abdelsamie, M.; Toney, M. F.; Bazan, G. C. Solvent Additives: Key Morphology-Directing Agents for Solution-Processed Organic Solar Cells. *Adv. Mater.* **2018**, *30*, 1707114–30.
- (12) Jaiswal, M.; Menon, R. Polymer Electronic Materials: A Review of Charge Transport. *Polym. Int.* **2006**, *55*, 1371–1384.
- (13) Zhang, S.; Zhang, J.; Abdelsamie, M.; Shi, Q.; Zhang, Y.; Parker, T. C.; Jucov, E. V.; Timofeeva, T. V.; Amassian, A.; Bazan, G. C.; Blakey, S. B.; Barlow, S.; Marder, S. R. Intermediate-Sized Conjugated Donor Molecules for Organic Solar Cells: Comparison of Benzodithiophene and Benzobis-thiazole-based Cores. *Chem. Mater.* 2017, 29, 7880–7887.